Hindawi
Advances in Materials Science and Engineering
Volume 2018, Article ID 2890931, 12 pages
https://doi.org/10.1155/2018/2890931

*Research Article*

# Effects of Imposed Damage on the Capillary Water Absorption of Recycled Aggregate Concrete

**Qi Gao,[1,2] Zhiming Ma,[1,3] Jianzhuang Xiao ,[1] and Fuan Li[2]**

[1]*Department of Structural Engineering, Tongji University, Shanghai 200092, China*
[2]*Xvchang Jinke Resource Recycling Co. Ltd, Xvchang 461000, China*
[3]*College of Civil Science and Engineering, Yangzhou University, Yangzhou 225127, China*

Correspondence should be addressed to Jianzhuang Xiao; jzx@tongji.edu.cn

Received 19 July 2018; Accepted 2 September 2018; Published 8 October 2018

Academic Editor: Behzad Nematollahi



Capillary water absorption of concrete is closely related to its pore structure, permeability, and durability. This paper intensively investigates the effects of imposed damage, including freeze-thaw damage and loading damage, on the capillary water absorption of recycled aggregate concrete (RAC). Freeze-thaw cycle test, loading test, and the experiment of capillary water absorption were carried out, respectively. The results demonstrate that the addition of recycled coarse aggregate (RCA) results in the increase in the capillary absorption behavior of RAC without imposed damage, and there exists a linear correlation between the behaviors of capillary water absorption and chloride penetration of RAC. The imposed freeze-thaw damage or load damage of RAC boosts with the increase of RCA replacement percentages after suffering the same freeze-thaw cycles or loading level. The imposed freeze-thaw damage and load damage further lead to the increase in the capillary water absorption of RAC, and the capillary absorption coefficient of RAC increases linearly with the increased RCA replacement percentages, after suffering the same freeze-thaw cycles or loading level. Furthermore, capillary absorption coefficient increases linearly with the growth of imposed freeze-thaw damage or load damage degree, which can be used to estimate the capillary absorption behavior of RAC exposed to the extreme environment.

## 1. Introduction

Construction and demolition waste (CDW) increased dramatically with the rapid development of the construction industry in the past few years, and the CDW will keep increasing at a high speed in China in the future [1, 2]. Traditional disposal of CDW is mainly the landfill and air storage, which requires more land occupation with a high cost. Due to the existence of hazardous substances in CDW, the traditional disposal of CDW also brings about a series of negative impacts on the environment, including soil, water, and atmosphere pollutions [3, 4]. Thereby, proposing an effective method to deal with the CDW is necessary. At the present stage, recycling waste concrete and bricks which account for about 80% of the CDW weight are the appropriate way to reduce the mass of CDW [2]. Recycled coarse aggregate (RCA) whose properties are similar to the natural coarse aggregate (NCA) can be produced through a series process of crushing and sieving, and the corresponding recycled aggregate concrete (RAC) is subsequently prepared, which can be used as the building materials. The properties of RAC have been investigated by the authors around the world, including the mechanical properties and some durability performance [5, 6]. Although the properties of RAC are inferior to the natural aggregate concrete (NAC), they can also be used in the engineering construction by the methods of mix optimization and design, such as increasing the amount of cement in the mix proportion.

Durability is the most important factor on the service life of concrete structures. Acting as the porous materials, water permeability is the main parameter of concrete durability, which is closely related to the carbonation, steel corrosion, freeze-thaw damage, and aggressive ions penetrations into concrete [7–9]. The high water permeability of concrete frequently results in the increase in the deterioration of concrete durability [10–12]. Water penetration into concrete

mainly depends on the force of capillary absorption and hydrostatic pressure, whereas the water-saturated state is difficult to reach except for the concrete exposed to the condition of high hydrostatic pressure, such as the deep sea environment; consequently, almost all of the water penetration into concrete is mainly by the force of capillary absorption, and the test of capillary water absorption is developed to evaluate the permeability of concrete [13, 14]. The capillary absorption force is mainly provided by the surface tension and pore absorption of concrete, which can well reflect the number and distribution of pores in concrete [15]. Due to the aggressive ions penetrating into concrete mainly by the medium of water penetration, there exists a correlation between the water and aggressive ions penetrations into concrete [16]. For example, when the concrete is exposed to the wet-dry environment (e.g., sea tidal zone), the capillary absorption provides the main driving force for the chloride and sulfate ions penetration into concrete.

Previous studies have investigated the capillary water absorption of NAC under various conditions. Wang, Bogas, and Hanžič have studied the capillary water absorption of NAC without imposed damage, and the results highlight that the mix proportion of concrete has an obvious effect on the capillary water absorption [15, 17, 18]. Furthermore, the capillary water absorption of NAC with imposed damage has also been investigated. Such as, Gonen presented the impact of freeze-thaw damage on the capillary absorption behavior of NAC [19], and Wang investigated the influence of applied loading on the capillary absorption behavior of NAC [20], which illustrates that the imposed freeze-thaw damage and load damage lead to the further increase in the capillary water absorption of NAC. The combination of capillary water absorption and imposed damage should be considered carefully in the evaluation and design of concrete durability.

A number of studies have been recently conducted to investigate the durability of RAC, and the focus was placed on chloride permeability, carbonation, freeze-thaw resistance, and so on, which highlights that the addition of RCA results in the decrease in the concrete durability [21–23]. However, there is currently a lack of adequate literature on the water permeability, especially for the capillary water absorption, of RAC. Attributing to the existence of the old mortar and interfacial transition zone (ITZ) with poor properties may lead to the increase in the capillary water absorption of RAC, considering the water penetration is frequently coupled with the freeze-thaw damage under cold condition, and RAC is inevitably exposed to the load application in the actual conditions, and the imposed damage may further increase the capillary water absorption of RAC. Consequently, the capillary water absorption of RAC with and without imposed damage should be investigated.

The aim of this paper is trying to experimentally investigate the capillary water absorption of RAC with and without imposed damage. Considering the practical service conditions, the effects of freeze-thaw damage and loading damage on the capillary water absorption of RAC were both investigated. Freeze-thaw cycle test, loading test, and capillary absorption experiment were carried out, respectively. Based on the testing results, the correlation between the capillary absorption behavior of RAC and RCA replacement percentages, as well as between the imposed damage and capillary absorption behavior of RAC, is established, which can be used to evaluate the capillary water absorption of RAC exposed to various conditions.

## 2. Experimental Program

*2.1. Mixture Proportions and Concrete Specimens.* Table 1 shows the properties of RCA and NCA, and the results confirm that the RCA has the inferior properties to NCA, due to the existence of old mortar which accounts for about 33% of the RCA weight. The packing density and apparent density of RCA are lower than those of NCA, and the RCA possesses the higher crushing value index compared with NCA. Particularly, the water absorption of RCA is about 5.3 times as high as that of NCA.

In order to investigate the effects of RCA replacement percentages on the capillary water absorption of RAC, different RCA replacement percentages are considered in the design of mix proportions, including 0%, 33%, 66%, and 100% of RCA to equivalently replace the NCA. Table 2 gives the specific mix proportions of RAC, and the specimen titled RAC-0% is also named as NAC, and the specimen titled RAC-33% presents the RCA replacement percentages are 33%. Polycarboxylate water-reducing agent produced in Shanghai was used, and all the slump values of various concrete mixes were kept around 90 mm by adjusting the amount of water-reducing agent in RAC. Attributing to high water absorption of RCA, the additional water was first mixed with the RCA to make the saturated surface dry, and the other binding materials, water as well as the water-reducing agent, were subsequently mixed to prepare the RAC. 100 mm cubes were used to measure the behavior of capillary water absorption, and the specimen with the size of $100 \times 100 \times 400\ \text{mm}^3$ was prepared to determine the relative dynamic modulus of concrete after different freeze-thaw cycles.

RAC specimens after hardening were moved into a curing room, where the temperature was kept at $(20 \pm 2)\ ^\circ\text{C}$ and the relative humidity was above 95%, for 28 days. The tests of freeze-thaw cycles and loading were conducted to induce the damage on RAC specimens, and then the capillary absorption test was carried out to investigate the capillary water absorption of concrete with and without imposed damage.

*2.2. Test of Capillary Water Absorption.* The water penetration into concrete is mainly by the force of capillary absorption when the concrete is in a relatively dry state. Capillary water absorption test was carried out according to the ASTM C1585 [24]. RAC specimens were first dried in the drying oven for 24 h where the temperature was kept around 105°C, and then the specimens were placed and cooled at room temperature. Finally, the capillary water absorption test was carried out, and the amount of absorbed water was determined at different time. Figure 1 describes the test of capillary water absorption and shows the SEM image of the

Table 1: Properties of RCA and NCA.

| Properties | | Recycled coarse aggregate (RCA) | Natural coarse aggregate (NCA) |
|---|---|---|---|
| Adhesive rate of old mortar | | 33% | 0% |
| Packing density (kg/m$^3$) | Loose packing density | 1280 | 1360 |
| | Tight packing density | 1440 | 1480 |
| Apparent density (kg/m$^3$) | | 2530 | 2660 |
| Crushing value index | | 11% | 5.13% |
| Clay content | | 1.8% | 0.8% |
| Water absorption | | 5.3% | 1.0% |

Table 2: Mix proportion of RAC (kg/m$^3$).

| Specimens | Water-binder ratio | Water | Cement | Sand | Natural aggregate | Recycled aggregate |
|---|---|---|---|---|---|---|
| RAC-0% | 0.5 | 180 | 360 | 650 | 1190 | 0 |
| RAC-33% | | | | | 797 | 393 |
| RAC-66% | | | | | 404 | 786 |
| RAC-100% | | | | | 0 | 1190 |

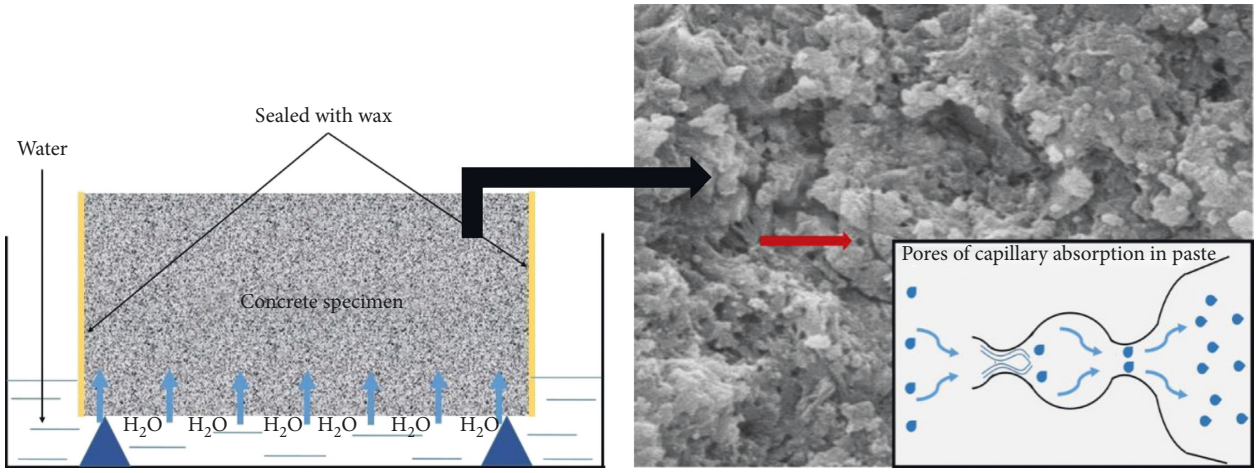


Figure 1: Capillary absorption test.

capillary absorption pores of concrete. There exists a mass of capillary pores, as well as the porous characteristics of CSH, which provides the capillary absorption force for water penetration into concrete.

If the gravity is neglected, the capillary absorption behavior can be described in a simple way by the following equations. In Equation (1), $\Delta W$ stands for the mass increase (g) of absorbed water by the surface area titled $S$ ($S$ = 100 mm × 100 mm), g/m$^2$. $A$ represents the coefficient of capillary absorption, g/(m$^2$·h$^{0.5}$), and it can be calculated by Equation (2) [25–27]. The amount of absorbed water and capillary absorption coefficient can well manifest the water permeability of cement-based materials, and the corresponding pores can be evaluated:

$$\Delta W = \frac{(m_1 - m_0)}{S}, \quad (1)$$

$$\Delta W = A\sqrt{t}. \quad (2)$$

The penetrations of water and chloride are both related to the pore structure, number, and distribution in cement-based materials. To investigate the relationship between the water and chloride penetrations into RAC, the maximum chloride content was determined by the test of capillary salt absorption at 5% NaCl solution for 24 h, and the chloride diffusion coefficient was also obtained by the free diffusion test at 5% NaCl solution for 30 d, in terms of Fick's second law.

*2.3. Test of Freeze-Thaw Cycles.* Accelerated freeze-thaw cycle test was carried out according to the Chinese Standard of "Testing code of concrete for port and waterway engineering" (JTJ 270), and one freeze-thaw cycle lasted for about four hours, and the core temperature of the concrete ranged from (8 ± 2) °C to (−17 ± 2) °C during one freeze-thaw cycle [28, 29]. RAC specimens were taken out from the setup of freeze-thaw cycles when the freeze-thaw cycles reached 0, 25, 50, and 75 times, respectively. The relative dynamic elastic modulus ($E_{rd}$) and mass loss were determined to quantitatively evaluate the imposed damage after different freeze-thaw cycles. Finally, the capillary absorption test of RAC with imposed freeze-thaw damage was

conducted, and the testing process was the same as the description in Section 2.1.

*2.4. Loading Test.* To investigate the imposed load damage on the capillary water absorption of RAC, different loading levels were first applied on the RAC, and the loading rate was 0.05 mm/min. The target load value was, respectively, 0%, 40%, 60%, and 80% of ultimate compressive strength ($f_c$), and the target load was kept for 60 min to make the RAC specimens obtain enough load damage. Subsequently, the specimens were unloaded, and the imposed load damage was determined by an ultrasonic concrete tester, and then the test of capillary water absorption was conducted according to Section 2.2. Figure 2 illustrates the loading test and the testing method of imposed load damage. The $E_{rd}$ is closely related to the cracks and pores development of cement-based materials, and it is frequently used in the performance evaluation of concrete with damage. The load damage degree can be determined according to Equation (3) by the change of the $E_{rd}$, where $D$ is the load damage degree, $E_{rd}$ presents relative dynamic elastic modulus, %, and $T_i$ and $T_0$ are the sonic time with and without imposed load [30, 31]:

$$D = 1 - E_{rd} = 1 - \frac{E}{E_0} = 1 - \left(\frac{T_0}{T_i}\right)^2. \quad (3)$$

## 3. Results and Discussions

*3.1. Capillary Water Absorption of RAC without Imposed Damage.* The compressive strength after 28 d and 56 d was first determined, and the results highlight that the addition of RCA leads to the decrease in the compressive strength of RAC. As shown in Figure 3, 33%, 66%, and 100% of RCA replacements result in 3.7%, 7.5%, and 12.9% decrease in the compressive strength of RAC after 28 d curing, and the results become 3.1%, 6.4%, and 13.6% after 56 d curing (Table 3).

Acting as the important parameters of concrete durability, the capillary absorption behavior is closely related to the composition, pore structure, and porosity of concrete. This section aims to investigate the capillary absorption behavior of RAC without any imposed damage. Figure 3(a) shows the capillary absorption curves of RAC with different RCA replacement percentages. The results reveal the amount of absorbed water rises with the increase of contact time with water, and the increased RCA replacement percentages result in the increase in the maximum amount of absorbed water of RAC. The capillary absorption coefficient increases with the rise of RCA replacement percentages; such as, the capillary absorption coefficient of RAC-33%, RAC-66%, and RAC-100% is about 1.08, 1.14, and 1.28 times as high as that of NAC. Furthermore, Figure 3(b) highlights the correlation between the capillary absorbed behavior and the RCA replacement percentages, and the results show that the capillary absorption coefficient of concrete increases linearly with the rise of RCA replacement percentages, and the specific equation is given in Equation (4), where $A_{\mathrm{RAC}}$ is the capillary absorption coefficient, g/(m$^2$·h$^{0.5}$), and $P_{\mathrm{RCA}}$ is the RCA replacement percentages, %:

$$A_{\mathrm{RAC}} = K_{\mathrm{cor}} \times P_{\mathrm{RCA}} + A_{\mathrm{NAC}} = 2.6 \times P_{\mathrm{RCA}} + 973.5. \quad (4)$$

Figure 4 illustrates the mechanism of water penetration into RAC and NAC. The significant difference between the RAC and NAC is the existence of old mortar and ITZ, and the old mortar possesses the inferior properties compared with new mortar, which provides more passageways for the water penetration into RAC. As shown in Figure 4, the obvious flaws, cracks, and pores can be seen from the SEM images of old ITZ and old mortar. Moreover, due to the existence of old mortar attached to RAC, the total mortar content per unit volume increases with the increase of the RCA replacement percentages, which also provides more capillary absorption pores for the water penetration into RAC. Consequently, the addition of RCA results in the increase in the capillary water absorption of concrete.

*3.2. Correlation between Chloride and Water Permeability of RAC.* Chloride penetration is the main reason that leads to the steel corrosion in reinforced concrete, which significantly reduces the concrete durability and structural safety [32–34]. The chloride and water penetrations into concrete are both related to the pore structures of concrete, and the chloride penetration into concrete is mainly by the medium of water penetration. Moreover, the capillary absorption coefficient and chloride diffusion coefficient, respectively, represent the water and chloride penetration rates. Table 4 shows the capillary water absorption and chloride penetration parameters of RAC, and the results highlight that the addition of RCA results in the increase in the penetration amount and penetration rate of water and chloride.

To investigate the correlation between the penetration behaviors of chloride and water, the relationship between the maximum absorbed water amount and the maximum chloride content, as well as the capillary absorption coefficient of water and diffusion coefficient of chloride, is described in Figures 5(a) and 5(b), and the results show that they follow a linear relation. Figure 5 also presents the specific equations, where the $W_{w,max}$ is the maximum amount of absorbed water, g/m$^2$; $W_{c,max}$ is the maximum chloride content, %; $D_{\mathrm{RAC}}$ is the chloride diffusion coefficient, $10^{-12}$ m$^2$/s; and $A_{\mathrm{RAC}}$ stands for the capillary water absorption coefficient, g/(m$^2$h$^{1/2}$). The evaluation and measurement of water permeability are easier than those of chloride permeability of concrete, and the correlation presented in this section gives a fast and effective method to estimate the chloride permeability of RAC by the change of water permeability.

*3.3. Capillary Water Absorption of RAC with Imposed Freeze-Thaw Damage.* Freeze-thaw damage frequently exists in concrete exposed to the cold condition, and it significantly reduces the impermeability, durability, and the service life of concrete [12, 35]. Gonen found that the freeze-thaw damage increases the capillary absorption behavior of NAC [19]. This

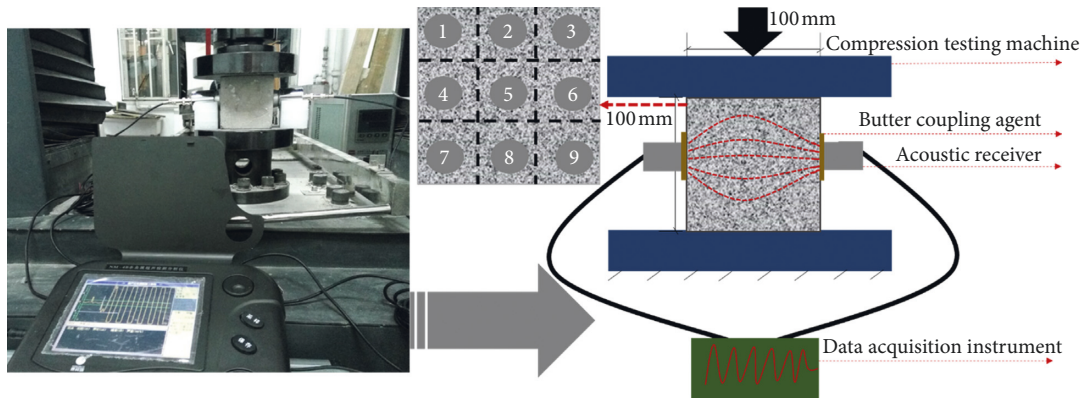


Figure 2: Loading test and test method of imposed load damage.

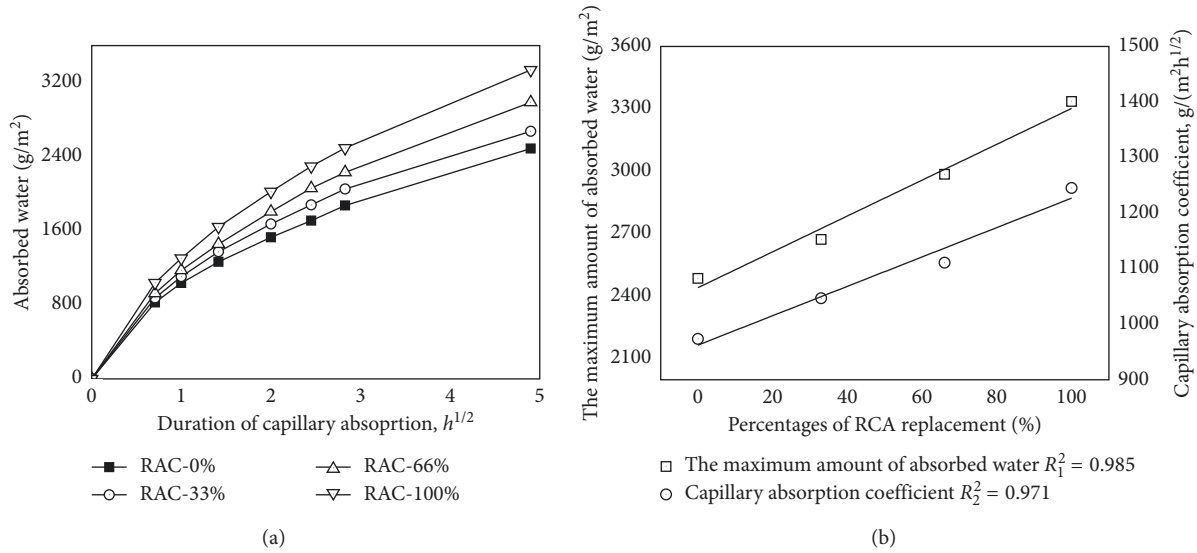


Figure 3: Capillary water absorption of RAC without imposed damage. (a) Capillary absorption curves of RAC with various RCA replacement percentages. (b) Correlation between capillary water absorption and RCA replacement percentages.

Table 3: Compressive strength of RAC after various curing days.

| Curing time | RAC-0% | RAC-33% | RAC-66% | RAC-100% |
|---|---|---|---|---|
| 28 d | 34.8 | 33.5 | 32.2 | 30.3 |
| 56 d | 38.9 | 37.7 | 36.4 | 33.6 |

section mainly investigates the effects of freeze-thaw damage on the capillary absorption behavior of RAC.

The mass loss and relative dynamic elastic modulus were first determined to present the freeze-thaw resistance of RAC, and the results are described in Figure 6. The mass loss of concrete increases with the increase of freeze-thaw cycles, and the addition of RCA results in the increase in the mass loss after the same freeze-thaw cycles; for example, the mass of RAC-0%, RAC-33%, RAC-66%, and RAC-100% after 75 freeze-thaw cycles decreases by 2.34%, 2.95%, 3.89%, and 5.45% compared with that without freeze-thaw attack. The relative dynamic elastic modulus ($E_{rd}$) of RAC decreases with the rise of freeze-thaw cycles, and the increased RCA replacement percentages result in decrease in the $E_{rd}$ of concrete after the same freeze-thaw cycles; such as, the $E_{rd}$ of RAC-0% is 1.15, 1.78, and 5.01 times as high as that of RAC-33%, RAC-66%, and RAC-100% after 75 freeze-thaw cycles.

The results mentioned above highlight that the RAC has the lower freeze-thaw resistance than NAC, and the freeze-thaw resistance decreases with the increase of RCA replacement percentages. Attributing to the existence of the old mortar adhered to RAC, the water adsorption of RAC increases with the increase of RCA replacement percentages, which leads to the RAC suffering more serious freeze-thaw expansion stress than NAC after the same freeze-thaw cycles. In addition, the cracks and pores in ITZ and old mortar of RCA are the weak points, which are easy to damage and aggravate the durability degradation of RAC. Consequently, the freeze-thaw damage of RAC increases with the increased RCA replacement percentage under the same condition of freeze-thaw cycles.

Capillary absorption curves of RAC after various freeze-thaw cycles are shown in Figure 7. The results highlight that the freeze-thaw damage results in the increase in the

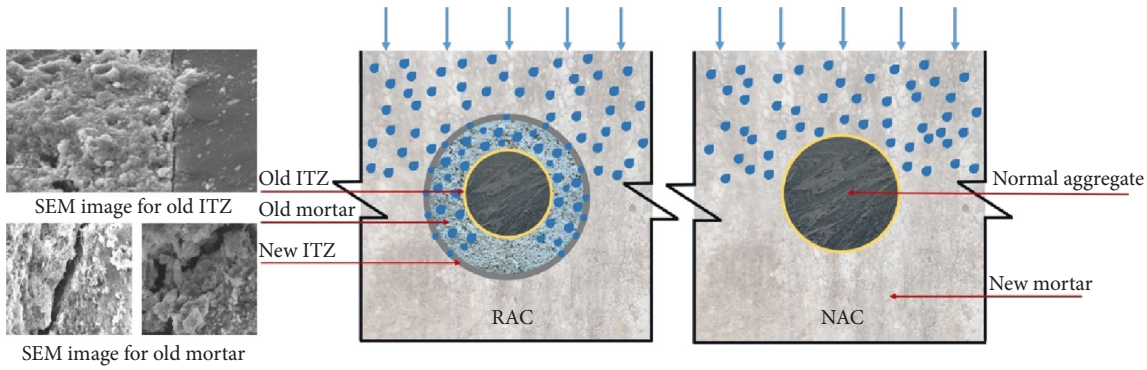


Figure 4: Mechanism of water penetration into RAC under the force of capillary absorption.

Table 4: Parameters of capillary water absorption and chloride penetrations.

| RCA replacement (%) | Capillary absorption parameters of water | | Chloride penetration parameters | |
|---|---|---|---|---|
| | The maximum amount of absorbed water, g/(m$^2$) | Capillary absorption coefficient, g/(m$^2$h$^{1/2}$) | The maximum amount of chloride (%) | Chloride diffusion coefficient, $10^{-12}$ m$^2$/s |
| 0 | 2486.67 | 973.5 | 0.1448 | 4.5076 |
| 33 | 2673.33 | 1046.6 | 0.162 | 5.7778 |
| 66 | 2986.67 | 1110.7 | 0.1797 | 6.1114 |
| 100 | 3336.67 | 1245.2 | 0.1922 | 6.8272 |

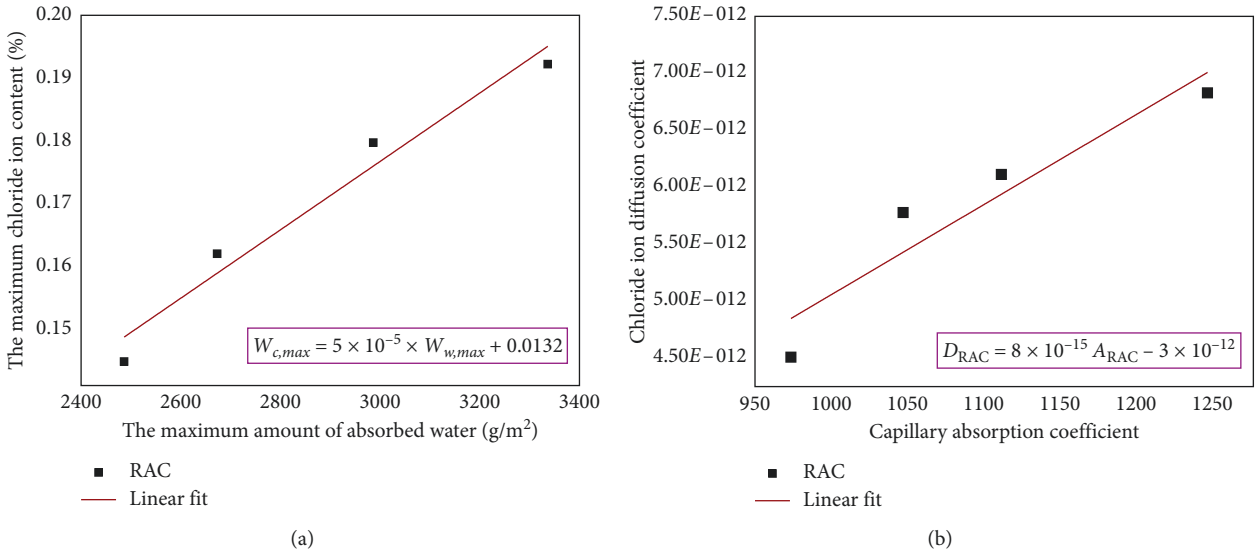


Figure 5: Correlation between capillary absorption behavior of water and chloride penetrations. (a) Relationship between the maximum amount of absorbed water and chloride content. (b) Relationship between capillary water absorption coefficient and chloride diffusion coefficient.

capillary water absorption of RAC. For example, the capillary absorption coefficient of NAC after suffering 75 freeze-thaw cycles is 0.94 times higher than that without freeze-thaw cycles, and the result is 6.29 times for RAC-100%. As more cracks and pores are formed and developed with the increase of freeze-thaw cycles, more passageways are provided for the water penetration into concrete.

By the mercury intrusion test (MIT), Table 5 gives the parameters of the pore structure of cement mortar with the w/c ratio of 0.5 after suffering different freeze-thaw cycles. It is remarkable that the amount of total porosity and the harmful pores quantity both rise with the increase of freeze-thaw cycles, which provides the passageway for the water penetration into concrete. Consequently, the absorbed water amount and capillary absorption coefficient of RAC both increase with the increase of freeze-thaw cycles.

As shown in Figures 7(a)–7(d), compared with the capillary absorption results of RAC with different RCA replacement percentages, it is easily found that the capillary

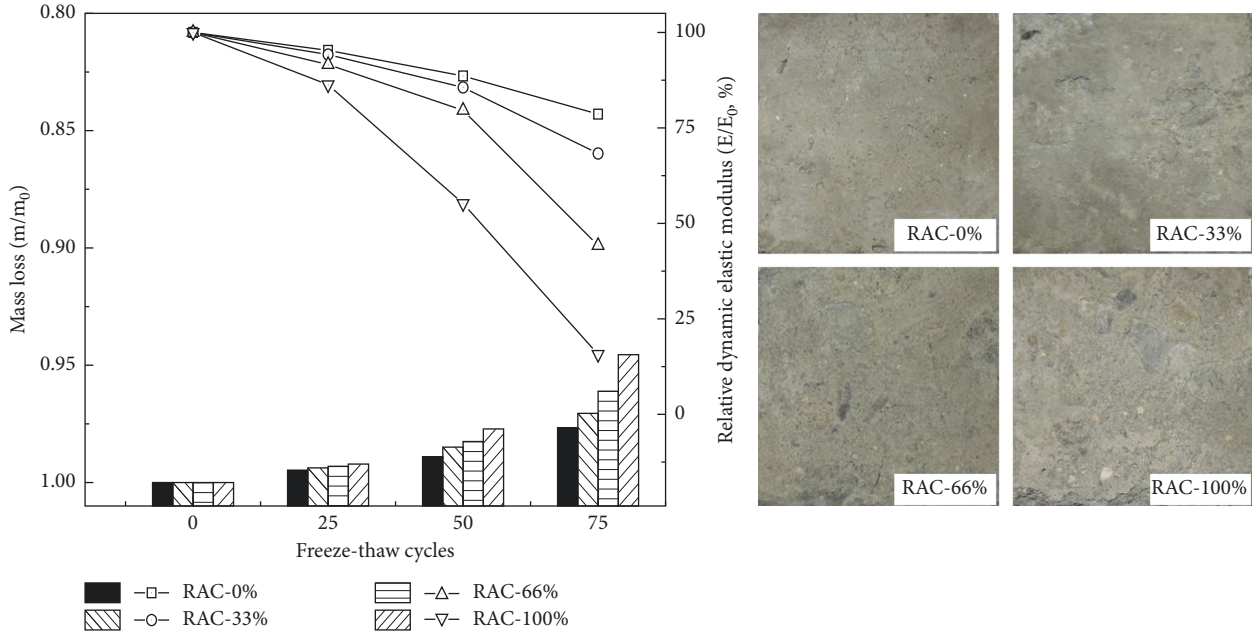


Figure 6: Mass loss and relative dynamic elastic modulus of RAC after freeze-thaw cycles.

absorption behavior of concrete increases with the increased RCA replacement percentages after the same freeze-thaw cycles, and the results become more obvious after suffering a large number of freeze-thaw cycles. Such as, the capillary absorption coefficient of RAC-33%, RAC-66%, and RAC-100% is, respectively, 1.10, 1.21 and 1.37 times as high as that of NAC after 25 freeze-thaw cycles, and the result becomes 1.62, 3.61, and 4.81 times after 75 freeze-thaw cycles. It can be explained that the cracks and pores caused by the freeze-thaw damage rise with the growing of RCA replacement percentages after suffering the same freeze-thaw cycles. The higher water content and low-quality RCA both aggravate the property degradation of RAC under freeze-thaw cycles. The $E_{rd}$ being closely related to the cracks and pores of concrete decreases by 21.4%, 31.7%, 55.8%, and 84.3% for RAC-0%, RAC-33%, RAC-66%, and RAC-100%, respectively, after 75 freeze-thaw cycles, as shown in Figure 6. Consequently, the capillary absorption behavior of RAC rises with the increase of RCA replacement percentages after the same freeze-thaw cycles. The results mentioned above highlight that the RAC has a higher capillary absorption behavior than NAC under the same condition of freeze-thaw cycles, and the increment becomes remarkable after suffering a large number of freeze-thaw cycles, which should be considered carefully in the durability design of RAC exposed to the cold environment:

$$A_{\mathrm{RAC}} = K_{\mathrm{cor}}^{\mathrm{FT}} \times \left(100 - \frac{E}{E_0}\right) + A_{\mathrm{RAC},0}. \quad (5)$$

Figure 8(a) shows the correlation among the suffered freeze-thaw cycles, RCA replacement percentages, and capillary absorption coefficient, which manifest the addition of RCA and suffered freeze-thaw cycles are found to have a negative effect on the capillary absorption behavior of RAC. For exploring the correlation between the imposed freeze-thaw damage and capillary absorption behavior of RAC, the relation between the $E_{rd}$ and capillary water absorption coefficient is established, which shows that the capillary water absorption coefficient increases linearly with the decrease of $E_{rd}$, as shown in Figure 8(b). The specific equation can be seen in Equation (5), where the $A_{\mathrm{RAC}}$ and $A_{\mathrm{RAC},0}$ is, respectively, the capillary absorption coefficient of RAC with and without imposed freeze-thaw damage, $\mathrm{g/(m^2h^{1/2})}$; $E/E_0$ stands for the relative dynamic elastic modulus, %; $K_{\mathrm{cor}}^{\mathrm{FT}}$ presents the correlation coefficient, and it is closed related to the RCA replacement percentage; the $K_{\mathrm{cor}}^{\mathrm{FT}}$ is 42 and 103 when the RCA replacement percentages are 0% and 100%, and $K_{\mathrm{cor}}^{\mathrm{FT}}$ with different RCA replacement percentages can be calculated by the method of linear insertion.

*3.4. Capillary Water Absorption of RAC with Imposed Loading Damage.* Through the observation of actual cracks development on the surface of RAC with different loadings, it can be seen that there existed some tiny cracks on the specimen surface when the applied loading reached 40%$f_c$, whereas the cracks continued to develop and the obvious cracks appear on the specimen surface when the applied loading reached 60%$f_c$; moreover, when the applied loading was 80%$f_c$, the width of crack became larger coupling with the spalling of concrete surface. Figure 9 shows the imposed load damage of RAC with various percentages of ultimate compressive strength. The results highlight that the increased loading results in the increase of damage degree of RAC, and the increasing range of load damage degree becomes more obvious when the applied loading is above 60%$f_c$. The damage level increases linearly with the growth of applied loading levels, and the increasing replacement percentage of RCA leads to the increase in the slope of fitting line. Such as,

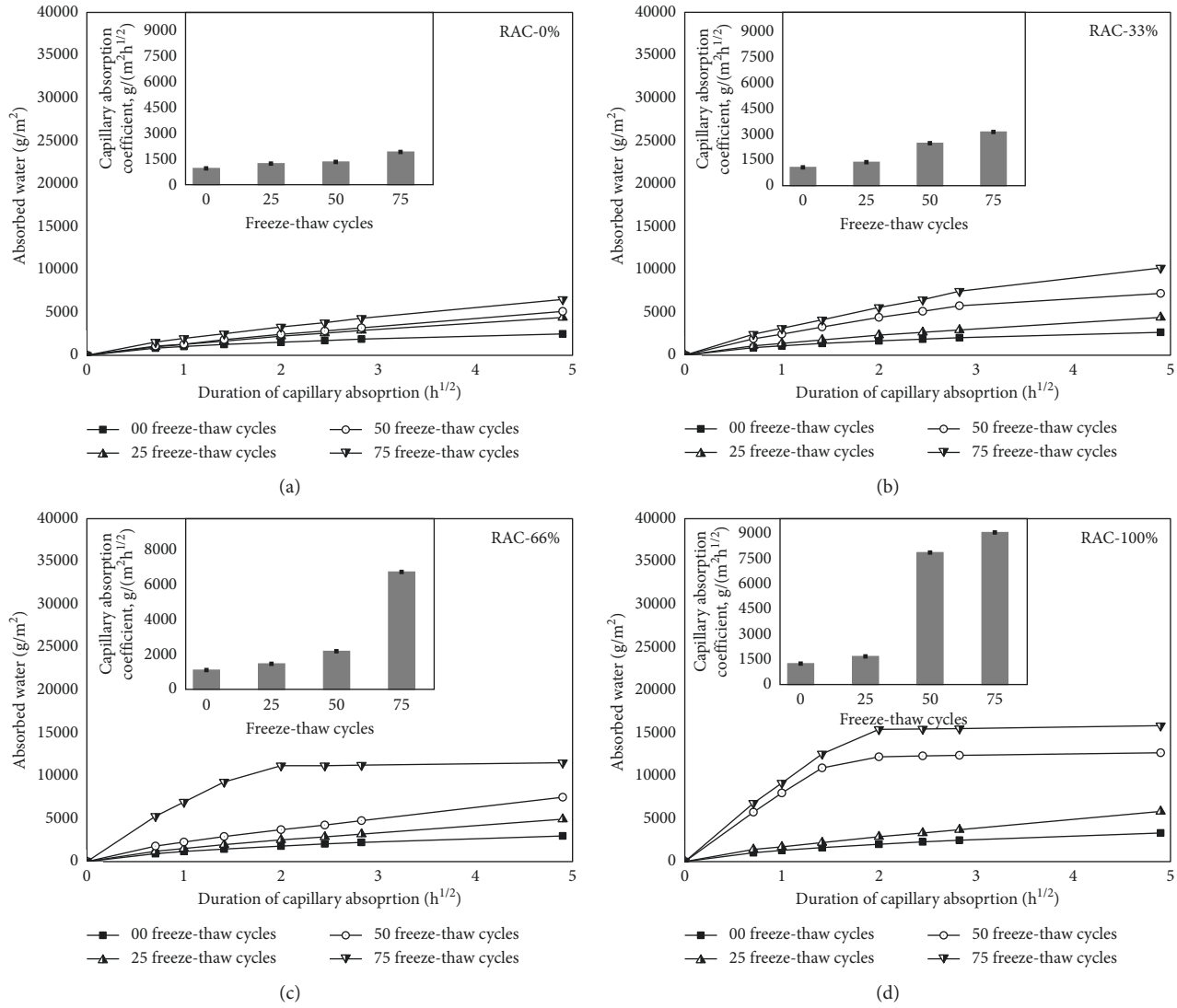


Figure 7: Capillary absorption curves of RAC after different freeze-thaw cycles. (a) RAC-0%, (b) RAC-33%, (c) RAC-66%, and (d) RAC-100%.

Table 5: Pore structure of cement mortar after various freeze-thaw cycles.

| Freeze-thaw cycles (times) | Total porosity (%) | Critical pores diameters (nm) | Graded volume of pore (ml/g) | | | |
|---|---|---|---|---|---|---|
| | | | Harmless pores <20.5 nm | Fewer harm pores 20.5–110 nm | Harmful pores 110–220 nm | Much harm pores >220 nm |
| 0 | 5.077 | 500 | 0.0090 | 0.0205 | 0.0082 | 0.0262 |
| 25 | 5.773 | 865 | 0.0101 | 0.0207 | 0.0086 | 0.0296 |
| 50 | 6.480 | 1551 | 0.0106 | 0.0214 | 0.0107 | 0.0380 |

the damage level of RAC-0% with the load of 40%$f_c$, 60%$f_c$, and 80%$f_c$ is, respectively, 0.020, 0.066, and 0.143, and the results become 0.047, 0.108, and 0.199 for RAC-100%.

As shown in Figure 9, the addition of RCA further results in the increase in the damage degree of RAC with the same loading, and the increasing range becomes more obvious with the increase of applied loading. For example, the damage degree of RAC-33%, RAC-66%, and RAC-100% is about 1.25, 1.95, and 2.40 times as high as that of RAC-0% when the applied loading is 40%$f_c$, and the results are 1.06, 1.31, and 1.40 times when the applied loading reaches 80%$f_c$. This could be attributed to the existence of RCA old mortar and ITZ with poor properties. On the one hand, the inferior properties of ITZ attached to RCA are easy to fail with the application of loading; on the other hand, the old mortar with a mass of initial damage cracks aggravates the property degeneration of RAC, which leads to the increase in the load damage degree of concrete with the addition of RCA.

Figure 10 presents the capillary absorption curves of RAC with different loadings, the results highlight that the

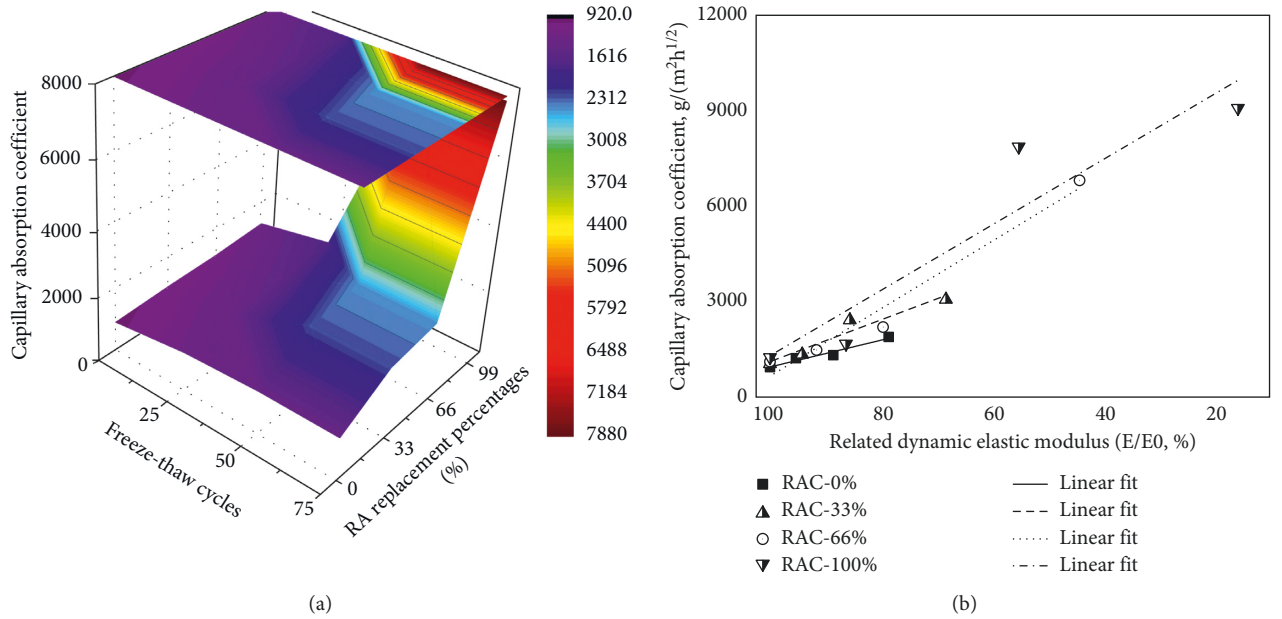


FIGURE 8: The relationship between the capillary water absorption and imposed freeze-thaw damage of RAC. (a) Correlation among suffered freeze-thaw cycles, RCA replacement percentages, and capillary absorption coefficient. (b) Correlation between capillary absorption coefficient and related dynamic elastic modulus ($E_{rd}$).

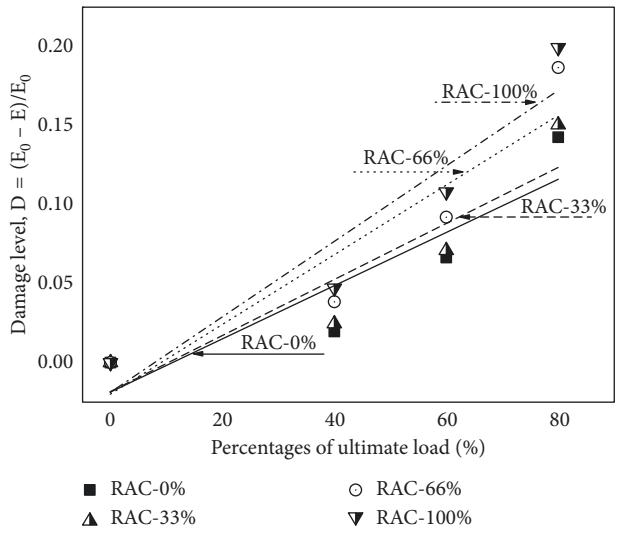


FIGURE 9: Imposed load damage of RAC with various percentages of ultimate compressive strength.

applied loading leads to the increase in the capillary water absorption of RAC, and the growth of capillary water absorption becomes significant when the applied loading is above 60%$f_c$. Such as, the capillary absorption coefficient of RAC-0% with the load of 0%$f_c$, 40%$f_c$, 60%$f_c$, and 80%$f_c$ is, respectively, 973.5 g/(m$^2$h$^{1/2}$), 1073.6 g/(m$^2$h$^{1/2}$), 1265.0 g/(m$^2$h$^{1/2}$), and 1649.1 g/(m$^2$h$^{1/2}$), and the results are 1245.2 g/(m$^2$h$^{1/2}$), 1326.4 g/(m$^2$h$^{1/2}$), 1788.4 g/(m$^2$h$^{1/2}$), and 2513.8 g/(m$^2$h$^{1/2}$) for RAC-100%. Comparing with the results in Figures 10(a)–10(d), the capillary absorption coefficient of concrete increases with the rise of RCA replacement percentages with the same loading; such as, the capillary absorption coefficient of RAC-33%, RAC-66%, and RAC-100% is, respectively, 1.04, 1.11, and 1.24 times as high as that of RAC-0% when the applied loading is 40%$f_c$, and the results become 1.09, 1.28, and 1.52 times when the applied loading reaches 80%$f_c$.

The results above highlight that the increased loading and RCA replacement percentages result in the increase in the capillary water absorption of concrete. This is attributed to the number of cracks rising with the increase of applied loading, which provides the passageways for water penetration into RAC; as a result, the applied loading increases the capillary water absorption of RAC. The cracks number and the mortar content per unit volume both increase with the rise of RCA replacement, which results in the capillary water absorption improvement of RAC with the same loading.

Figure 11 shows the relationship between capillary absorption coefficient and RCA replacement percentages with different loading levels, and the results manifest that the capillary absorption coefficient increases linearly with the rise of RCA replacement percentages with the same loading; however, the increased loading results in the increases in the slope of fitting line. To investigate the correlation between the capillary water absorption and imposed load damage, the relationship between the capillary absorption coefficient and load damage degree ($D$) is established, and the results are described in Figure 12:

$$A^{L}_{RAC} = k^{L}_{cor} \times D + A_{RAC,0}. \quad (6)$$

The results highlight that the capillary absorption coefficient increases linearly with the rise of $D$; furthermore, the slope of fitting line grows with the increase of RCA replacement percentages. Equation (6) shows the specific

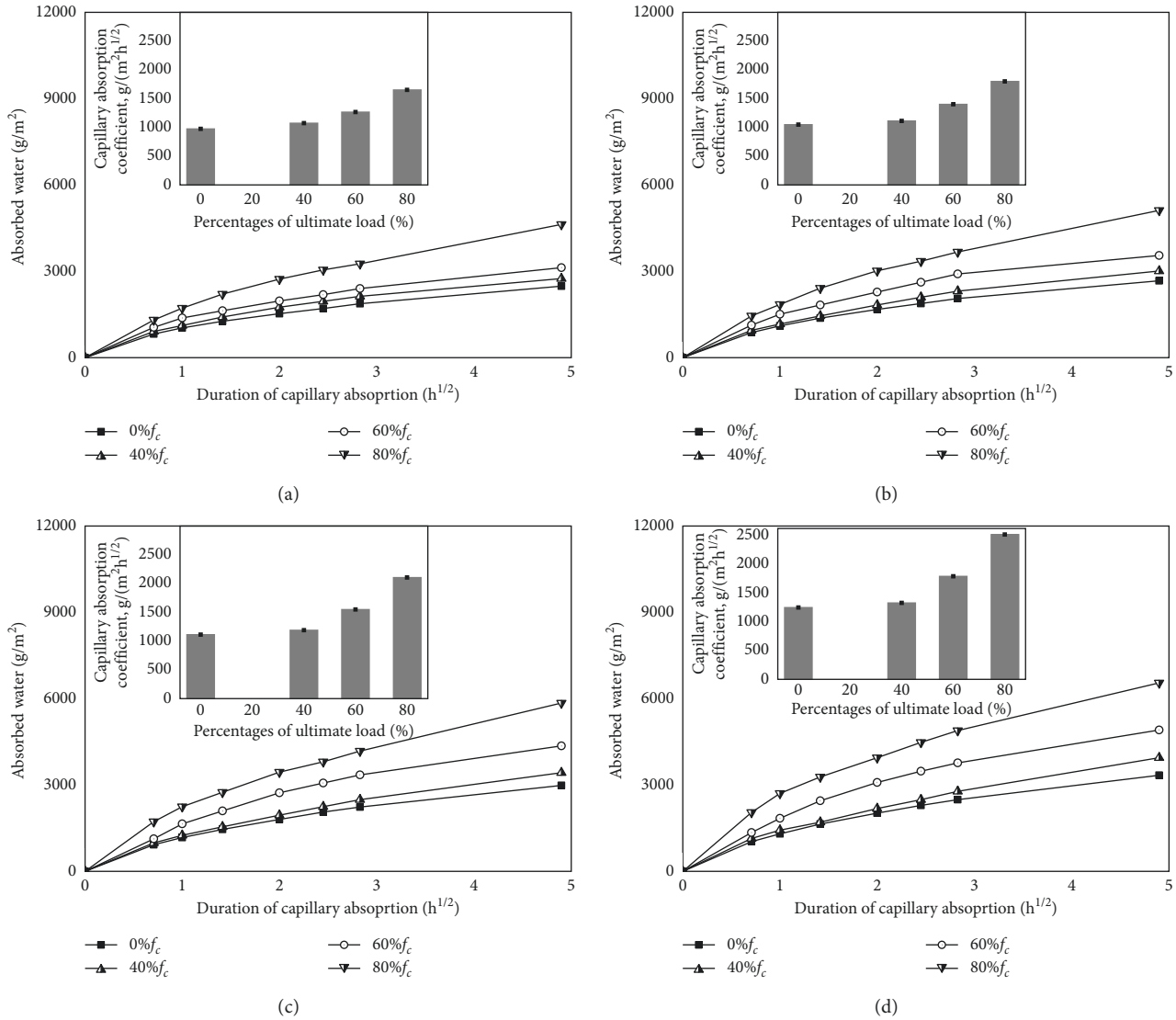


Figure 10: Capillary absorption curves of RAC with different loadings. (a) RAC-0%, (b) RAC-33%, (c) RAC-66%, and (d) RAC-100%.

equation, where the $D$ is the load damage degree; $A_{RAC,0}$ and $A^{L}_{RAC}$ are, respectively, the capillary absorption coefficient of RAC without and with imposed loading damage, (g/m$^2$h$^{1/2}$); and $k^{L}_{cor}$ stands for the correlation coefficient, and it is closely related to the RCA replacement percentages, the $K^{ET}_{cor}$ is, respectively, 4480 and 6640 when the RCA replacement percentages is 0% and 100%, and $K^{FT}_{cor}$ with the other RCA replacement percentages can be calculated by the method of linear insertion. Although the relationship between the capillary water absorption of RAC and imposed loading damage is established after unloading, the capillary water absorption of RAC with sustained loading can also be estimated by the value of damage degree with sustained loading using Equation (6).

This paper investigates the capillary water absorption of RAC with and without imposed damage, whereas there still has some shortcomings need to be solved in the further study. For example, if the source of RCA is much completed, the relation between the various sources of RCA and the capillary absorption behavior of RAC should be investigated. The method of improving the water permeability resistance of RAC should be also studied, such as by the waterproof treatment and mix optimization, which is necessary for the wide application of RAC in the engineering construction.

## 4. Conclusions

This paper investigates the capillary absorption behavior of RAC with different replacement percentages of RCA under normal, freeze-thaw cycles and loading conditions, respectively. Based on the results of this experimental work, the following conclusions can be drawn:

(1) As the old mortar adhered to RCA possesses a low quality and the mortar content per unit volume of concrete increases with the growing of the RCA replacement percentages, the capillary water

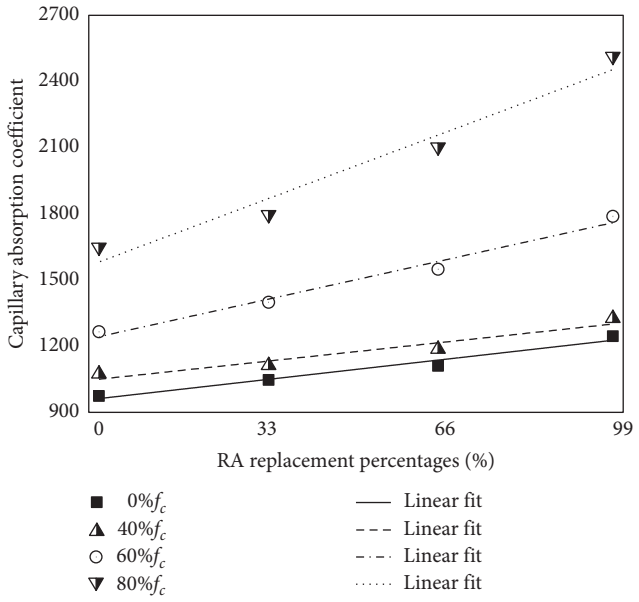


Figure 11: Relationship between capillary absorption coefficient and RCA replacement percentages.

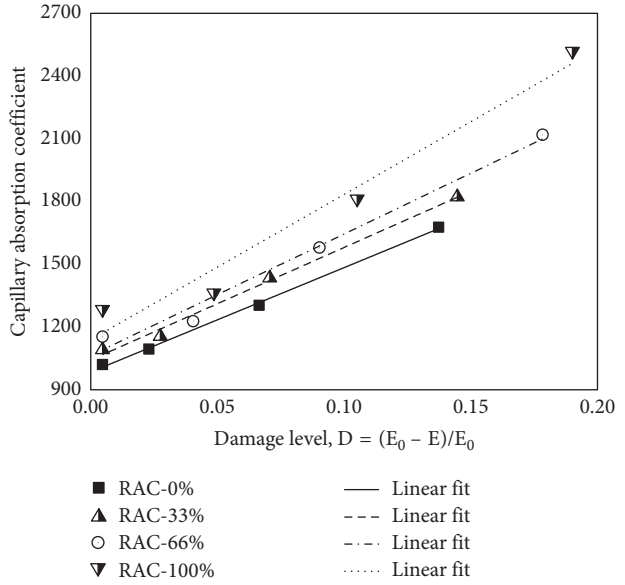


Figure 12: Correlation between capillary absorption coefficient and imposed load damage (D).

absorption of concrete increases with the increased RCA replacement percentages under normal condition. The capillary absorption coefficient and RCA replacement percentages follow a linear correlation. Furthermore, the addition of RCA results in the decrease in the compressive strength. There exists a linear relation between the capillary water absorption coefficient and chloride diffusion coefficient, as well as the maximum amount of absorbed water and chloride content, which provides an effective way to estimate the chloride permeability through the behavior of capillary water absorption of RAC.

(2) Exposing to the condition of freeze-thaw cycles, the freeze-thaw resistance of concrete decreases with the increase of the RCA replacement percentage. The imposed freeze-thaw damage results in the increase in the capillary absorption behavior of RAC. Capillary water absorption of concrete increases with the rising of RCA replacement percentages after the same freeze-thaw cycles, and the increase becomes more obvious after suffering a large number of freeze-thaw cycles. Moreover, there exists a linear correlation between the capillary absorption coefficient and imposed freeze-thaw damage ($E_{rd}$).

(3) Under the condition of applied loading, the imposed loading damage boosts with the increasing of applied loading, and the addition of RCA results in the increase in the imposed damage of concrete with the same loading level. The applied loading leads to the increase in the capillary water absorption of RAC, and the increasing range becomes more obvious with the applied loading above 60%$f_c$. Particularly, the capillary water absorption increases linearly with the growth of imposed loading damage, which can be used to estimate the capillary absorption behavior of RAC with imposed loading damage.

(4) The addition of RCA and imposed damage both results in the increase in the capillary water absorption of concrete, which should be considered in the durability design. Considering the high capillary water absorption of RCA, they can act as the water storage materials used in the construction of sponge city.

## Data Availability

The data used to support the findings of this study are available from the corresponding author upon request.

## Conflicts of Interest

The authors declare that they have no conflicts of interest.

## Acknowledgments

The authors wish to acknowledge the financial support from the National Natural Science Foundation of China (NSFC) (nos. 51438007 and 5161101205) and China-Japanese Joint Program sponsored by Ministry of Science and Technology in China (no. 2016YFE0118200).

## References

[1] H. Yuan and L. Shen, "Trend of the research on construction and demolition waste management," *Waste Management*, vol. 31, no. 4, pp. 670–679, 2011.

[2] J. Z. Xiao, Z. M. Ma, T. B. Sui, A. Akbarnezhad, and Z. H. Duan, "Mechanical properties of concrete mixed with recycled powder produced from construction and demolition

waste," *Journal of Cleaner Production*, vol. 188, no. 2, pp. 720–731, 2018.

[3] P. Mercader-Moyano and A. RamãRez-De-Arellano-Agudo, "Selective classification and quantification model of C & D waste from material resources consumed in residential building construction," *Waste Management and Research*, vol. 31, no. 5, pp. 458–74, 2013.

[4] N. Seror, S. Hareli, and B. A. Portnov, "Evaluating the effect of vehicle impoundment policy on illegal construction and demolition waste dumping: Israel as a case study," *Waste Management*, vol. 34, no. 8, pp. 1436–1445, 2014.

[5] M. Cao, H. Zhang, and X. U. Ling, "Research progress on deformation performance of recycled concrete," *Materials Review*, vol. 28, no. 1, pp. 106–109, 2014.

[6] M. Safiuddin, U. J. Alengaram, M. M. Rahman, M. A. Salam, and M. Z. Jumaat, "Use of recycled concrete aggregate in concrete: a review," *Journal of Civil Engineering and Management*, vol. 19, no. 6, pp. 796–810, 2013.

[7] T. Gonen and S. Yazicioglu, "The influence of compaction pores on sorptivity and carbonation of concrete," *Construction and Building Materials*, vol. 21, no. 5, pp. 1040–1045, 2007.

[8] Rasheeduzzafar, "Influence of cement composition on concrete durability," *ACI Materials Journal*, vol. 89, no. 6, pp. 574–586, 1992.

[9] Z. M. Ma, T. J. Zhao, J. Z. Xiao, and P. G. Wang, "Effect of applied loads on water and chloride penetrations of strain hardening cement-based composites," *Journal of Materials in Civil Engineering*, vol. 28, no. 9, pp. 1–12, 2016.

[10] J. J. Shi and W. Sun, "Effects of phosphate on the chloride-induced corrosion behavior of reinforcing steel in mortars," *Cement and Concrete Composites*, vol. 45, pp. 166–175, 2014.

[11] M. Basista and W. Weglewski, "Chemically assisted damage of concrete: a model of expansion under external sulfate attack," *International Journal of Damage Mechanics*, vol. 18, no. 2, pp. 155–175, 2009.

[12] W. Li, M. Pour-Ghaz, J. Castro, and J. Weiss, "Water absorption and critical degree of saturation relating to freeze-thaw damage in concrete pavement joints," *Journal of Materials in Civil Engineering*, vol. 24, no. 3, pp. 299–307, 2012.

[13] W. H. Dunagan, "Methods for measuring the passage of water through concrete," *Proceedings of the American society for Testing Materials*, vol. 39, pp. 866–880, 1939.

[14] Z. M. Ma, T. J. Zhao, and Y. D. Zhao, "Effects of hydrostatic pressure on chloride ion penetration into concrete," *Magazine of Concrete Research*, vol. 68, no. 17, pp. 1–10, 2016.

[15] L. Hanžič, L. Kosec, and I. Anžel, "Capillary absorption in concrete and the Lucas–Washburn equation," *Cement and Concrete Composites*, vol. 32, no. 1, pp. 84–91, 2010.

[16] H. J. Du, H. J. Gao, and S. D. Pang, "Improvement in concrete resistance against water and chloride ingress by adding graphene nanoplatelet," *Cement and Concrete Composites*, vol. 83, no. 1, pp. 114–123, 2016.

[17] L. Wang and T. Ueda, "Mesoscale modeling of water penetration into concrete by capillary absorption," *Ocean Engineering*, vol. 38, no. 4, pp. 519–528, 2011.

[18] J. A. Bogas, M. G. Gomes, and S. Real, "Capillary absorption of structural lightweight aggregate concrete," *Materials and Structures*, vol. 48, no. 9, pp. 2869–2883, 2014.

[19] T. Gonen, S. Yazicioglu, and B. Demirel, "The influence of freezing-thawing cycles on the capillary water absorption and porosity of concrete with mineral admixture," *KSCE Journal of Civil Engineering*, vol. 19, no. 3, pp. 667–671, 2015.

[20] L. C. Wang and S. Li, "Capillary absorption of concrete after mechanical loading," *Magazine of Concrete Research*, vol. 66, no. 8, pp. 420–431, 2014.

[21] W. H. Kwan, M. Ramli, K. J. Kam, and M. Z. Sulieman, "Influence of the amount of recycled coarse aggregate in concrete design and durability properties," *Construction and Building Materials*, vol. 26, no. 1, pp. 565–573, 2012.

[22] H. B. Liu, J. Sun, and X. H. Cong, "A review of the durability of recycle aggregate concrete," *Applied Mechanics and Materials*, vol. 744–746, pp. 1357–1360, 2015.

[23] J. Z. Xiao, D. Lu, and J. W. Ying, "Durability of recycled aggregate concrete: an overview," *Journal of Advanced Concrete Technology*, vol. 11, no. 12, pp. 347–359, 2013.

[24] ASTM C1585, *Standard Test Method for Measurement of Rate of Absorption of Water by Hydraulic-Cement Concretes*, ASTM International, West Conshohocken, PA, USA, 2013.

[25] S. A. Kelham, "A water absorption test for concrete," *Magazine of Concrete Research*, vol. 40, no. 143, pp. 106–110, 1988.

[26] F. H. Wittmann, A. D. A. Wittmann, and P. G. Wang, "Capillary absorption of integral water repellent and surface impregnated concrete," *Restoration of Buildings and Monuments*, vol. 20, no. 4, pp. 281–290, 2014.

[27] D. Wang, P. Yang, P. K. Hou, L. Zhang, Z. Zhou, and X. Cheng, "Effect of $SiO_2$ oligomers on water absorption of cementitious materials," *Cement and Concrete Research*, vol. 87, pp. 22–30, 2016.

[28] Z. M. Ma, F. Z. Zhu, and T. J. Zhao, "Effects of surface modification of silane coupling agent on the properties of concrete with freeze-thaw damage," *KSCE Journal of Civil Engineering*, vol. 22, pp. 657–669, 2018.

[29] JTJ270, *Testing Code of Concrete for Port and Waterway Engineering*, Ministry of Communications of PRC, Beijing, China, 1998.

[30] F. Z. Zhu, J. Liu, and Z. L. Li, "Discussion on the influence of water content in concrete dynamic elastic modulus test," *Concrete*, vol. 277, pp. 40–56, 2012.

[31] Q. X. Luo and J. H. Bungey, "Using compression wave ultrasonic transducers to measure the velocity of surface waves and hence determine dynamic modulus of elasticity for concrete," *Construction and Building Materials*, vol. 10, no. 4, pp. 264–270, 1996.

[32] J. W. Ying, *Chloride Ion Diffusion Law and Basic Characteristics of Recycled Aggregates Concrete*, Doctoral dissertation, Tongji University, Shanghai, China, 2013.

[33] K. Thangavel and N. S. Rengaswamy, "Relationship between chloride hydroxide ratio and corrosion rate of steel in concrete," *Cement and Concrete Composites*, vol. 20, no. 4, pp. 283–292, 1998.

[34] C. G. Berrocal, K. Lundgren, and I. Löfgren, "Corrosion of steel bars embedded in fibre reinforced concrete under chloride attack: state of the art," *Cement and Concrete Research*, vol. 80, pp. 69–85, 2016.

[35] M. Saito, M. Ohta, and H. Ishimori, "Chloride permeability of concrete subjected to freeze-thaw damage," *Cement and Concrete Composites*, vol. 16, no. 4, pp. 233–239, 1994.